Proceedings of the
47th IEEE Conference on Decision and Control
Cancun, Mexico, Dec. 9-11, 2008

A Nonlinear, Control-oriented Model for Ionic Polymer-Metal Composite Actuators

Zheng Chen, Dawn Rochelle Hedgepeth and Xiaobo Tan

Abstract— **Ionic polymer-metal composites (IPMCs) form an important category of electroactive polymers and have many potential applications in biomedical, robotic and micro/nano manipulation systems. In this paper, a nonlinear, control-oriented model is proposed for IPMC actuators. A key component in the proposed model is the nonlinear capacitance of IPMC. A nonlinear partial differential equation (PDE), which can capture the fundamental physics in IPMC, is fully considered in the derivation of nonlinear capacitance. A systems perspective is taken to get the nonlinear mapping from the voltage to the induced charge by analytically solving the nonlinear PDE at the steady state when a step voltage is applied. The nonlinear capacitance is incorporated into the circuit model, which includes additionally the pseudocapacitance due to the electrochemical adsorption process, the ion diffusion resistance, and the nonlinear DC resistance of the polymer, to capture electrical dynamics of IPMC. With electromechanical coupling, the curvature output is derived based on the circuit model. The proposed model is formulated in the state space, which will be the starting point for nonlinear controller design. Experimental verification shows that the proposed model can capture the major nonlinearities in the electrical response of IPMC.**

I. INTRODUCTION

Ionic polymer-metal composites (IPMCs) form an important category of electroactive polymers (also known as artificial muscles) and have built-in actuation and sensing capabilities [1]. An IPMC sample typically consists of a thin ion-exchange membrane (e.g., Nafion), chemically plated on both surfaces with a noble metal as electrodes. When a voltage is applied across an IPMC, transport of hydrated cations and water molecules within the membrane and the associated electrostatic interactions lead to bending motions, and hence the actuation effect. Because of their softness, resilience, biocompatibility and the capability of producing large deformation under a low action voltage, IPMCs are very attractive materials for many applications in the fields of biomedical devices and biomimetic robots [2].

An accurate and practical mathematical model is desirable in the application of IPMC. Extensive work has been done in modeling of IPMC. Current modeling work can be classified into three categories based on their complexity levels. Based purely on the empirical responses, *black-box* models, e.g., [3], offer minimal insight into the governing mechanisms within the IPMC. As a more detailed approach, the gray-box models, e.g., [4], are partly based on physical principles while also relying on empirical results to define some of the more complex physical processes. In the most complex form, white-box models with partial differential equations (PDEs), e.g., [5], attempt to explain the underlying physics for the sensing and actuation responses of IPMCs, but they are not practical for real-time control purposes. Bufalo *et al.* applied mixture theory to the modeling of IPMC actuators [6], but they only addressed the behavior under quasi-static actuation. Chen and Tan [7] bridged the gap between the empirical models and the physical models by exactly solving the governing PDEs in the Laplace domain, and came up with an infinite-dimensional transfer function relating the output to the input. However, this control-oriented model was based on a linear PDE which ignored the nonlinear terms in the physical model. This approximation only holds when a small voltage is applied. A nonlinear model is needed when a relatively high voltage is applied to the IPMC to generate large deformation.

Nonlinear behaviors of IPMC have been reported in literature. Chen *et al*. [8] employed the Preisach operator to capture the hysteresis in IPMC. Bonomo [9] reported a nonlinear circuit model of IPMC. However, it is an empirical nonlinear model and cannot capture the fundamental physics in IPMC. Nemat-Nasser [10] captured a nonlinear capacitance of IPMC with an assumption that there is asymmetric charge distribution along the thickness direction and that cation-depleted layer forms near the anode side when a relatively high voltage is applied. However, the region without cation depletion was still governed by the linear PDE.

Our proposed model is based on the original nonlinear PDE, which can capture ion diffusion, water migration, and electrostatic interactions in IPMC. The modeling work starts from the analysis of the equilibrium of IPMC under a step voltage input, which can be captured by a nonlinear ordinary differential equation (ODE). Numerical analysis of the nonlinear ODE demonstrates an asymmetric charge distribution along the thickness direction. The nonlinear term in the original PDE cannot be ignored when a moderate voltage (> 0.2V) is applied. Since the nonlinear ODE cannot be explicitly solved, a systems perspective is taken to derive the analytical nonlinear mapping from the voltage to the charge. It is verified by the numerical solution, and is practically useful in real-time control.

A nonlinear circuit model is employed to capture the electrical dynamics of IPMC. It incorporates nonlinear capacitance of IPMC derived from the nonlinear mapping function between the charge and the voltage, ion diffusion resistance, pseudocapacitance due to the electrochemical process at the

Z. Chen, D. R. Hedgepeth and X. Tan are with the Smart Microsystems Laboratory, Department of Electrical & Computer Engineering, Michigan State University, East Lansing, MI 48824, USA. chenzhe1@egr.msu.edu, hedgepe1@msu.edu, xbtan@egr.msu.edu

polymer-metal interface [11], and nonlinear DC resistance of the polymer [9]. Based on the electromechanical coupling effect, the curvature output can be obtained from the electrical dynamic model. The proposed model shows consistency with the linear model when the voltage is small [5]. With definition of state variable, input, and output, the proposed model is formulated in the state space, which will be the starting point for nonlinear control design. Parameters are measured or identified through experiments. The proposed model is validated in experiments.

The remainder of the paper is organized as follows. The governing nonlinear PDE is reviewed in Section II. Section III shows numerical and analytical analysis of the nonlinear PDE at the steady state. In Section IV, a nonlinear circuit model is introduced to capture the electrical dynamics of IPMC. The derivation of curvature output of IPMC and a nonlinear control-oriented model are also shown in Section IV. Experimental validation of the proposed model is presented in Section V. Finally, concluding remarks are provided in Section VI.

II. GOVERNING NONLINEAR PDE

The governing PDE for charge distribution in an IPMC was first presented in [5] and then used by Farinholt and Leo [12] for investigating the actuation and sensing response. Let $\mathbf{D}$, $\mathbf{E}$, ϕ, and ρ denote the electric displacement, the electric field, the electric potential, and the charge density, respectively. The following equations hold:

$$\mathbf{E} = \frac{\mathbf{D}}{\kappa_e} = -\nabla\phi \ , \tag{1}$$

$$\nabla \cdot \mathbf{D} = \rho = F(C^+ - C^-) \ , \tag{2}$$

where κ_e is the effective dielectric constant of the polymer, F is Faraday's constant, and C^+ and C^- are the cation and anion concentrations, respectively. Since the thickness of an IPMC is much smaller than its length or width, one can assume that $\mathbf{D}$ and $\mathbf{E}$ are restricted to the thickness direction only. Fig. 1 shows the geometrics definition of IPMC.

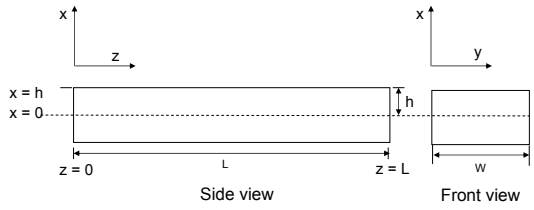

Fig. 1. Geometric definitions of an IPMC beam.

The continuity expression relates the ion flux to the cation concentration,

$$\frac{\partial J}{\partial x} = -\frac{\partial C^+}{\partial t}. \tag{3}$$

The flux of ion movement and water migration is

$$J = -\frac{dk_e}{F}\left(\frac{\partial^2 E}{\partial x^2} - \frac{F(1-C^-\Delta V)}{RT}E\left(\frac{\partial E}{\partial x} + \frac{FC^-}{k_e}\right)\right). \tag{4}$$

where d is the ionic diffusivity, R is the gas constant, T is the absolute temperature, ΔV is the volumetric change. With the continuity equation (3), one can derive the nonlinear governing PDE in terms of the electric field,

$$\frac{\partial^2 E}{\partial t \partial x} = d\Big(\frac{\partial^3 E}{\partial x^3} - \frac{F(1-C^-\Delta V)}{RT}\Big[\frac{\partial^2 E}{\partial x^2}\cdot E + \Big(\frac{\partial E}{\partial x}\Big)^2\Big] - \frac{F^2 C^-(1-C^-\Delta V)}{RTk_e}\frac{\partial E}{\partial x}\Big). \tag{5}$$

Many papers [5], [10], [12], [7] have mentioned that the nonlinear term involving $\frac{\partial E}{\partial x}\cdot E$ can be ignored in (4) based on the assumption

$$\rho(x) = k_e\frac{\partial E}{\partial x} << C^- F, \tag{6}$$

and come up with a linear PDE,

$$\frac{\partial \rho}{\partial t} - d\frac{\partial^2 \rho}{\partial x^2} + \frac{F^2 dC^-}{\kappa_e RT}\left(1 - C^-\Delta V\right)\rho = 0 \ . \tag{7}$$

However, this assumption will not hold when a relatively high voltage is applied, as to be shown later in this paper.

III. ANALYSIS OF PDE IN STEADY STATE

The key component in the model is the capacitance of the IPMC. The first step of modeling work is to analyze the nonlinear PDE at equilibrium when a step voltage is applied, and find the mapping function from voltage to charge. At equilibrium, $J = 0$, which implies

$$E''(x) - aE'(x)E(x) - bE(x) = 0, \tag{8}$$

where $E'(x) = \frac{dE(x)}{dx}$ and $E''(x) = \frac{d^2E(x)}{dx^2}$ and

$$a \triangleq \frac{F(1-C^-\Delta V)}{RT}, \quad b \triangleq \frac{F^2 C^-(1-C^-\Delta V)}{RTk_e}.$$

The following two conditions hold for the ODE:

1) The overall charge-balance condition leads to

$$E(h) = E(-h). \tag{9}$$

2) The potential difference is equal to the applied voltage

$$\int_{-h}^{h} E(x)\,dx = V. \tag{10}$$

Note that $x = -h$ is defined as the anode and $x = h$ is defined as the cathode in this section, so $V \geqslant 0$.

There are two approaches to solving the nonlinear ODE (8), numerical solution and analytical solution. The numerical solution can show the charge distribution, electrical field, electrical potential along x direction. The analytical solution can provide a mapping function from voltage to charge, leading to the nonlinear capacitance of IPMC. These two approaches will be discussed next.

A. Numerical solution of PDE at the steady state

In order to numerically solve the second-order ODE (8), one needs to know the boundary condition $E(-h)$ and $E'(-h)$, or $E(h)$ and $E'(h)$. However, these conditions are unknown. So we change the initial point to $x = x_0$, where x_0 is defined as the zero charge density point, $\rho(x_0) = k_e E'(x_0) = 0$. Note that x_0 will also depend on the applied voltage.

In order to satisfy the conditions (9) and (10), we run the following steps recursively:

Step 1: Assign a value to x_0 such that $-h < x_0 < +h$, and a very small value to $E(x_0) = E_0$;

Step 2: Integrate ODE (8) forward from $x = x_0$ to $x = h$ and backward from $x = x_0$ to $x = -h$, separately, to get $E(x)$ and $E'(x)$;

Step 3: If $|E(-h) - E(h)| \leqslant \varepsilon$, go to Step 4; If $E(-h) - E(h) > \varepsilon$, decrease $x_0 = x_0 - \varepsilon_1$ and go to Step 2; if $E(-h) - E(h) < -\varepsilon$, increase $x_0 = x_0 + \varepsilon_1$ and go to Step 2;

Step 4: Integrate $-\int_{-h}^{x} E(x)\,dx$ to get $\phi(x)$ with $\phi(-h) = 0$;

Step 5: If $|\phi(h) + V| < \varepsilon_2$, go to Step 6; If $\phi(h) + V > \varepsilon_2$, increase $E_0 = E_0 + \varepsilon_3$ and go to Step 1; If $\phi(h) + V < -\varepsilon_2$, decrease $E_0 = E_0 - \varepsilon_3$ and go to Step 1;

Step 6: Calculate $\rho(x) = k_e E'(x)$ and integrate $Q = \int_{x_0}^{h} \rho(x)\,Sdx$, then stop.

In the steps above, ε, ε_1, ε_2 are small positive constants, and $S = WL$ is the surface area of IPMC. All the physical parameters in the PDE are listed in Table I in Section V. Fig. 2 shows the numerical simulation results when $V = 2.61$V. Fig 2(a) shows the asymmetric charge distribution along the thickness direction. Two inset figures show the details at the turning points of the curve. The negative charge density near the anode approaches the saturation value $C^- F$. The charge density distribution also shows that (6) will not hold in the region close to the boundaries. In other words, the linear PDE will not hold when a relatively high voltage is applied.

Numerical solution offers us insight into the charge distribution, electrical field and electrical potential along the thickness direction for a given step voltage, but it does not provide us an overall picture of the induced charge versus applied voltage. Moreover, the numerical solution takes recursive steps to find proper initial conditions, and requires much computation which is not practical for control purposes. An analytical solution is practical in real time implementation. It is also the starting point in the derivation of nonlinear capacitance of IPMC.

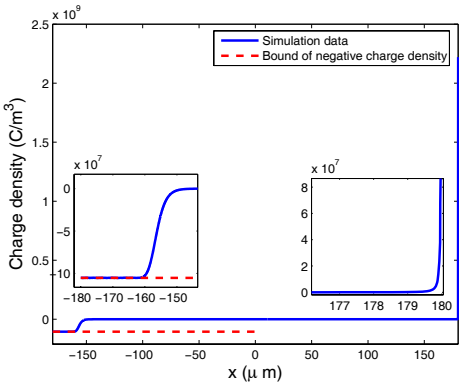

Fig. 2. Numerical simulation of charge density for $V = 2.61$V.

B. Analytical solution of PDE at the steady state

Define $y \triangleq E$ and $p \triangleq E'$. Eq. (8) becomes

$$\frac{pdp}{(ap+b)} = ydy. \tag{11}$$

We integrate both sides of (11). On the left-hand side, we integrate from $p(x_0)$ to p, while on the right-hand side, we integrate from $E(x_0)$ to y:

$$\frac{p}{a} - \frac{b}{a^2}\ln\left(\frac{a}{b}p+1\right) = \frac{1}{2}y^2 - \frac{E(x_0)^2}{2}. \tag{12}$$

Since it is difficult to solve (12) to get p in terms of y, one cannot continue to solve the ODE to get an explicit function $E(x)$. We take a systems perspective to solve this problem. What we are really concerned about is how the total charge is analytically related to the voltage input. Thus it is not necessary to know the explicit function $E(x)$.

By integrating both sides of (8) from $x = -h$ to $x = h$, we get

$$E'(h) - E'(-h) - \frac{a}{2}\left(E^2(h) - E^2(-h)\right) - bV = 0. \tag{13}$$

From (9) and (13), one can get

$$V = \frac{1}{b}(E'(h) - E'(-h)). \tag{14}$$

The total charge Q can be obtained by integrating $\rho(x)$ from $x = x_0$ to $x = h$, where $\rho(x_0) = 0$:

$$\int_{x_0}^{h} \rho(x)\,Sdx = Q = (E(h) - E(x_0))\,Sk_e. \tag{15}$$

In Section III-A, Fig. 2(b) shows that $E(x_0) << E(h)$ ($E(x_0) = 1.5 \times 10^{-23}$ and $E(h) = 2 \times 10^7$). So (15) can be written as

$$E(h) = E(-h) = \frac{Q}{Sk_e}. \tag{16}$$

Note that $E'(h)$ and $E'(-h)$ are the positive root and negative root of (12), respectively, when $y = E(h)$.

Define

$$k \triangleq \frac{1}{2}\left(\frac{Q}{Sk_e}\right)^2. \tag{17}$$

Then (12) can be written as

$$\frac{p}{a} - k = \frac{b}{a^2}\ln\left(\frac{a}{b}p+1\right). \tag{18}$$

Theorem 3.1: If $k > 0$, there exist two roots (p_1, p_2) for (18) such that $-\frac{b}{a} < p_1 < 0$ and $p_2 > 0$. Furthermore, if $k = 0$, then $p_1 = p_2 = 0$.

Proof: Define

$$\chi(p) = \frac{p}{a} - \frac{b}{a^2}\ln\left(\frac{a}{b}p+1\right) - k, \quad p > -\frac{b}{a}. \tag{19}$$

Let's start with the case when $k > 0$. Because $\chi(0) = -k < 0$, $\chi(p)$ is continuous in $(-\frac{b}{a}, +\infty)$ and

$$\lim_{p\to+\infty} \chi(p) = +\infty > 0, \qquad \lim_{p\to-\frac{b}{a}} \chi(p) = +\infty > 0,$$

there exist $p_1 \in (-\frac{b}{a},0)$, $p_2 \in (0,+\infty)$ such that $\chi(p_1)=0$ and $\chi(p_2)=0$. Since

$$\chi'(p)=\frac{p}{ap+b}, \tag{20}$$

with $p>-\frac{b}{a}$, we can get $\chi'(p)>0$ when $p>0$ and $\chi'(p)<0$ when $0>p>-\frac{b}{a}$. So $\chi(p)$ is monotonically increasing in $(0,+\infty)$, and monotonically decreasing in $(-\frac{b}{a},0)$. Then p_1 and p_2 should be unique. When $k=0$, $\chi(0)=0$, implying $p_1=p_2=0$. ■

In order to get the mapping function from V to Q, we need find out how k is related to the distance of two roots $|p_1-p_2|$. As shown in Fig 3, the roots of (18) are the intersection points (p_1 and p_2) of the following two curves:

$$\begin{aligned}\eta &= \frac{b}{a^2}\ln\left(\frac{a}{b}p+1\right)=f(p),\\ \eta &= \frac{p}{a}-k=\lambda(p).\end{aligned}$$

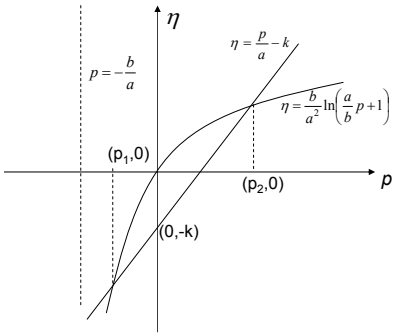

Fig. 3. Illustration of solving for p_1 and p_2.

From Fig. 3, the negative root p_1 will never hit the line $p=-\frac{b}{a}$ because $p=-\frac{b}{a}$ is the asymptote of the logarithmic function of $\eta=\ln(\frac{b}{a}p+1)$. The physical explanation of this is the following. Since the negative ions cannot move and the negative ion density are uniform in IPMC, $\frac{b}{ak_e}=C^-F$ is the bound of the negative charge density. So $p>-\frac{b}{a}$ implies that the layer of depletion of positive charges will not form, although the positive charge density can be very close to zero.

Then with (14), we can solve (18) to get

$$k=\overline{\Gamma}(V)\triangleq\begin{cases}\Gamma(V), V>0\\ 0, V=0\end{cases} \tag{21}$$

where

$$\Gamma(V)\triangleq\frac{b}{a^2}\left(\frac{aV}{e^{aV}-1}-\ln\left(\frac{aV}{e^{aV}-1}\right)-1\right), \tag{22}$$

With l'Hospital's rule, $\lim_{V\to 0}\Gamma(V)=0$. So k is a continuous function of V. With (17) and (21), one can get the total charge Q in function of V

$$Q=Sk_e\sqrt{2\overline{\Gamma}(V)}. \tag{23}$$

When $V\to 0$, one can approximate $\overline{\Gamma}(V)\approx\frac{b|V|^2}{8}$ using its Taylor series expansion around $V=0$, then $Q\approx\frac{\sqrt{b}VSk_e}{2}$, which is consistent with the charge in the linear case [5].

Fig. 4 shows the simulation results of charge versus voltage at the steady state. It includes the simulation results based on analytical solution of the nonlinear ODE, numerical solution of the nonlinear ODE and numerical solution of the linear ODE (which ignores the nonlinear term). One can see that the analytical solution can match the numerical solution well. When the voltage is small, one can ignore the nonlinear term in the nonlinear PDE. However, if a relatively large voltage is applied, the error between the nonlinear model and the linear one becomes significant. The above analytical analysis of PDE at the steady state will be helpful for deriving the nonlinear capacitance of IPMC, which will be discussed next.

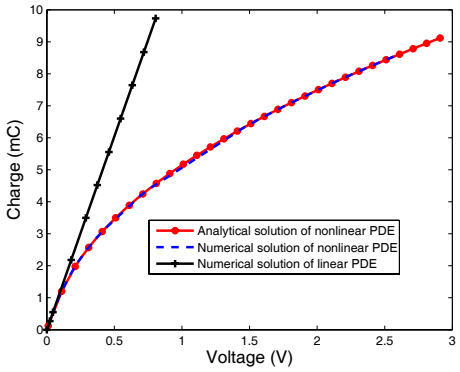

Fig. 4. Charge versus voltage at the steady state.

IV. NONLINEAR CIRCUIT MODEL

The above analysis can only capture the nonlinear capacitance of IPMC. A dynamic model needs to capture the transient processes in IPMC. Bonomo [9] employed a nonlinear circuit model to capture the electrical dynamics of IPMC. However, it is only an empirical model. In this paper, a nonlinear circuit model is also employed (Fig. 5), but it is physics-based. It incorporates the nonlinear capacitance of IPMC C_1, pseudocapacitance C_a due to the electrochemical adsorption process at the polymer-metal interface, ion diffusion resistance R_c, electrode resistance R_a, and nonlinear DC resistance of polymer R_{dc}.

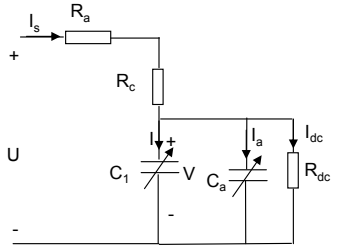

Fig. 5. Circuit model of IPMC.

A. Nonlinear capacitance of IPMC

The nonlinear capacitance can be obtained by taking derivative of (23),

$$C_1(V)=\frac{dQ}{dV}=Sk_e\frac{\Gamma'(V)}{\sqrt{2\Gamma(V)}}, \tag{24}$$

where $\Gamma'(V)$ is the first derivative of $\Gamma(V)$. From (22),

$$\Gamma'(V) = \frac{b}{a}\left(1 - \frac{e^{aV}-1}{aV}\right)\frac{e^{aV}-1-aVe^{aV}}{(e^{aV}-1)^2}. \quad (25)$$

The proposed analytical solution of nonlinear capacitance captures the fundamental physics in the IPMC. It is represented by a function in terms of physical parameters and dimensions, and is geometrically scalable.

B. Pseudocapacitance due to adsorption

For an electrochemical surface process, e.g., the so-called underpotential deposition of H [13], the following holds:

$$\mathrm{M} + \mathrm{H_3O^+} + e \overset{\mathrm{K}}{\rightleftharpoons} \mathrm{MH_{ads}} + \mathrm{H_2O}, \quad (26)$$

where M is the substrate (usually a noble metal, Pt, Rh, Ru or Ir). Since IPMC has Pt as electrode and some electrolyte in the polymer, the underpotential deposition process should be incorporated into the model [11]. The adsorption current due to this electrochemical process can be represented by [13]:

$$I_a = C_a(V)\frac{dV}{dt}, \quad (27)$$

where

$$C_a(V) \triangleq \frac{q_1 SF}{RT}\frac{K_1 c^{H+} e^{-\frac{VF}{RT}}}{(K_1 c^{H+} + e^{-\frac{VF}{RT}})^2}, \quad (28)$$

q_1 is some constant (For H on polycrystalline Pt, $q_1 = 210\,\mu\mathrm{C/cm^2}$ [13]), $K_1 = \frac{k_1}{k_{-1}}$, k_1, k_{-1} are the chemical rate constants for forward and reverse directions of (26), and c^{H+} is the concentration of H^+.

C. Nonlinear DC resistance

The current response under a step voltage input will not vanish at the steady state [9] because of the DC resistance of polymer. One can approximate the nonlinear DC current by a series of polynomial functions $Y(V)$. In this paper, we use a third-order polynomial function:

$$I_{dc} = \mathrm{sign}(V)(Y_1|V| + Y_2|V|^2 + Y_3|V|^3) \overset{\Delta}{=} Y(V). \quad (29)$$

Note that I_{dc} is supposed to be an odd function of V. That's why $\mathrm{sign}(V)$ appears in (29).

D. Curvature output

The stress is proportional to the charge density $\sigma = \alpha_0\rho$ [5], where α_0 is the coupling constant. The moment generated by IPMC can be derived as:

$$M = W\alpha_0 k_e\left(\mathrm{sign}(V)\,2h\sqrt{2\overline{\Gamma}(|V|)} - V\right). \quad (30)$$

If one takes $V \to 0$,

$$M \to W\alpha_0 k_e V\left(h\sqrt{b} - 1\right) \approx W\alpha_0 k_e V h\sqrt{b}, \quad (31)$$

which is consistent with the moment reported in the linear case [5]. With (30), one can then obtain the curvature output

$$\kappa = \Psi(V) \overset{\Delta}{=} \frac{3\alpha_0 k_e\left(\mathrm{sign}(V)\,2h\sqrt{2\Gamma(|V|)} - V\right)}{2Y_e h^3}. \quad (32)$$

where Y_e is the equivalent Young's modulus of IPMC.

E. Nonlinear control-oriented model

The objective of this work is to derive a control-oriented nonlinear model which can be used in controller design. Based on the circuit model (Fig. 5) and the curvature output (30), the model structure is shown in Fig. 6.

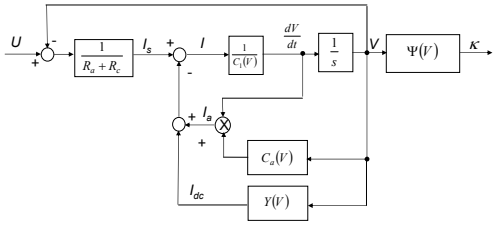

Fig. 6. Model structure.

From (27) and (29), one can get

$$\frac{dV}{dt} = \frac{\frac{U-V}{R_a+R_c} - Y(V)}{C_1(V) + C_a(V)}. \quad (33)$$

Defining the state variable $x = V$, the control input $u = U$, and the system output $y = \kappa$, one can obtain a first-order nonlinear dynamic model in the state space:

$$\begin{aligned} \dot{x} &= -\frac{x + Y(x)(R_a+R_c) - u}{(C_1(x) + C_a(x))(R_a+R_c)}, \\ y &= \Psi(x). \end{aligned} \quad (34)$$

V. EXPERIMENTAL VERIFICATION

Some physical parameters can be directly measured through the experiments, such as temperature T, dimensions L, W, h, equivalent Young's modulus of IPMC Y_e, electrodes resistance R_a. Some parameters are physical constants, such as R, F, q_1. Other parameters $(Y_1, Y_2, Y_3, R_c, K_1, C^-, k_e, \alpha_0)$ can be identified by a model fitting process.

The current responses under a series of step voltage inputs are measured in order to identify those unmeasured parameters. Fig. 7 shows the initial current and DC currents in the current step response. The initial current I_{s0} is the current when the capacitors are uncharged ($V = 0$). The DC current $I_{s\infty}$ is the current when the capacitors have been fully charged. When $V = 0$, from Fig. 6, one can get

$$I_{s0} = \frac{U}{R_a + R_c}. \quad (35)$$

Fig. 7(a) shows that the initial current is a linear function of step voltage. One can obtain the linear resistance $R_a + R_c$ by calculating the slope of I_{s0} versus U. Fig. 7 shows that the DC current can be approximated by a third-order polynomial function of V (29), thus the coefficients Y_1, Y_2, Y_3 can be identified. c^{H+}, K_1, k_e can be tuned to fit the transient process with the model. Fig. 8 shows the current responses under 1.0 V. One can conclude that the proposed model can capture both the transient process and the steady state in current responses under step voltage inputs. Identification of α_0 was reported in [7]. Table I shows all the parameters in the model.

The model is further verified through an experiment to examine the current response under a sinusoid voltage input

TABLE I

PARAMETERS IN THE MODEL.

F	R	T	Ra
96487 C/mol	8.3143 J/mol · K	300 K	18 Ω
Rc	L	W	h
48 Ω	22 mm	10 mm	100 μm
C^-	κ_e	c^{H+}	K_1
1091 mol/m^3	1.34×10^{-6} F/m	1×10^{-6} mol/m^3	4×10^5
α_0	Y_e	q_1	
0.129 J/C [7]	0.56 GPa [7]	210 μC/cm^2 [13]	
Y_1	Y_2	Y_3	
1×10^{-5} A/V	1×10^{-4} A/V^2	1×10^{-4} A/V^3	

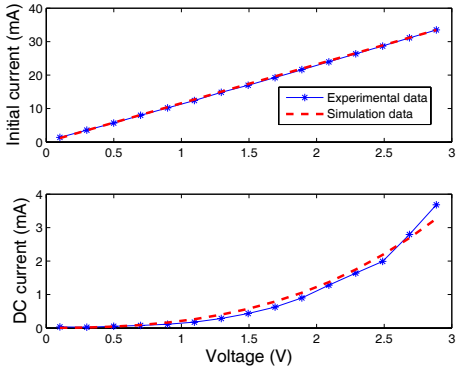

Fig. 7. Initial current and DC current versus voltage step.

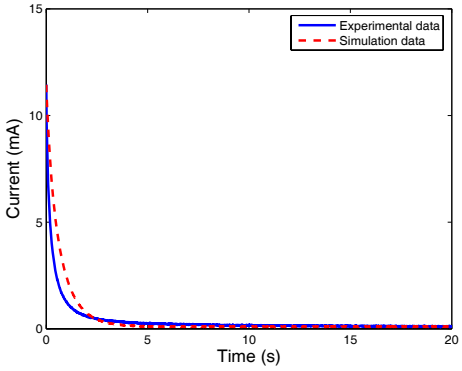

Fig. 8. Current response under step voltage input of 1.0 V.

with frequency 0.01 Hz and amplitude 3 V. Fig. 9 shows that the model can predict the current response well.

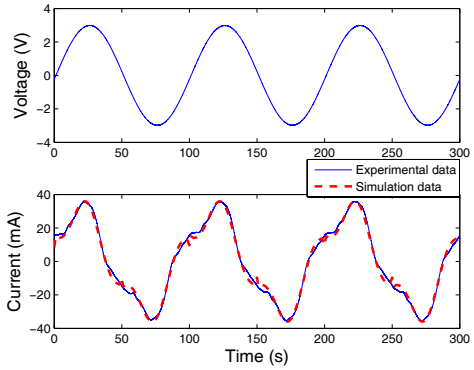

Fig. 9. Current response under a sinusoid voltage input.

VI. CONCLUSIONS AND FUTURE WORK

In this work, a nonlinear, control-oriented model is proposed for IPMC actuation. It is derived based on the nonlinear dynamics-governing PDE. Numerical analysis of the nonlinear PDE at the steady state shows an asymmetric charge distribution along the thickness. A systems perspective is taken in analytical analysis of nonlinear PDE to obtain a nonlinear mapping from the voltage to the induced charge, which represents the nonlinear capacitance of IPMC. A nonlinear circuit model is employed to capture the electrical dynamics of IPMC, including the nonlinear capacitance of IPMC, the ion diffusion resistance, the pseudocapacitance due to the electrochemical process at the polymer-metal interface, and nonlinear DC resistance of polymer. The proposed model is described in the state space, which will be the starting point of nonlinear control of IPMC. The proposed model is validated experimentally by the electrical responses of IPMC.

Future work will be focused on the following: 1) incorporating mechanical dynamics into the model; 2) design of nonlinear controller and nonlinear system analysis; 3) application to IPMC-actuated biomedical devices and biomimetic robots which require large deformation of IPMC.

ACKNOWLEDGMENTS

This research was supported in part by an NSF CAREER grant (ECCS 0547131), and by MSU IRGP (05-IRGP-418).

REFERENCES

[1] M. Shahinpoor and K. Kim, "Ionic polymer-metal composites: I. Fundamentals," *Smart Materials and Structures*, vol. 10, pp. 819–833, 2001.

[2] X. Tan, D. Kim, N. Usher, D. Laboy, J. Jackson, A. Kapetanovic, J. Rapai, B. Sabadus, and X. Zhou, "An autonomous robotic fish for mobile sensing," in *Proceedings of the IEEE/RSJ International Conference on Intelligent Robots and Systems*, Beijing, China, 2006, pp. 5424–5429.

[3] R. Kanno, A. Kurata, S. Tadokoro, T. Takamori, and K. Oguro, "Characteristics and modeling of ICPF actuator," *Proceedings of the Japan-USA Symposium on Flexible Automation*, pp. 219–225, 1994.

[4] K. M. Newbury and D. J. Leo, "Electromechanical modeling and characterization of ionic polymer benders," *Journal of Intelligent Material Systems and Structures*, vol. 13, pp. 51–60, 2002.

[5] S. Nemat-Nasser and J. Li, "Electromechanical response of ionic polymer-metal composites," *Journal of Applied Physics*, vol. 87, no. 7, pp. 3321–3331, 2000.

[6] G. D. Bufalo, L. Placidi, and M. Porfiri, "A mixture theory framework for modeling the mechanical actuation of ionic polymer metal composites," *Smart Materials and Structures*, vol. 10, pp. 1–14, June 2008.

[7] Z. Chen and X. Tan, "A control-oriented and physics-based model for ionic polymer-metal composite actuators," *IEEE/ASME Transactions on Mechatronics*, 2008, In press.

[8] Z. Chen, X. Tan, and M. Shahinpoor, "Quasi-static positioning of ionic polymer-metal composite (IPMC) actuators," in *Proceedings of the IEEE/ASME International Conference on Advanced Intelligent Mechatronics*, Monterey, CA, 2005, pp. 60–65.

[9] C. Bonomo, L. Fortuna, P. Giannone, S. Graziani, and S. Strazzeri, "A nonlinear model for ionic polymer metal composites as actuators," *Smart Materials and Structures*, vol. 16, pp. 1–12, 2007.

[10] S. Nemat-Nasser, "Micromechanics of actuation of ionic polymer-metal composites," *Journal of Applied Physics*, vol. 92, no. 5, pp. 2899–2915, 2002.

[11] B. J. Akle, "Characterization and modeling of the ionomer-conductor interface in ionic polymer transducers," Ph.D. dissertation, Virginia Polytechnic Institute and State University, 2005.

[12] K. M. Farinholt, "Modeling and characterization of ionic polymer transducers for sensing and actuation," Ph.D. dissertation, Virginia Polytechnic Institute and State University, 2005.

[13] B. E. Conway, *Electrochemical Supercapacitors Scientific Fundamentals and Technological Applications*. Springer, 1999.